HHS Public Access

Author manuscript

Nat Cell Biol. Author manuscript; available in PMC 2012 March 01.

Published in final edited form as:

Nat Cell Biol. ; 13(9): 1062–1069. doi:10.1038/ncb2316.

miRNA-mediated feedback inhibition of JAK/STAT morphogen signaling establishes a cell fate threshold

Wan Hee Yoon[1], **Hans Meinhardt**[2], and **Denise J. Montell**[1,*]

[1]Department of Biological Chemistry, Center for Cell Dynamics, Johns Hopkins University School of Medicine, 855 North Wolfe St., Suite 450, Baltimore, MD 21205, USA

[2]Max-Planck-Institut für Entwicklungsbiologie, Spemannstrasse 35, D-72076 Tübingen, Germany

Patterns of cell fates generated by morphogens are critically important for normal development, yet the mechanisms by which graded morphogen signals are converted into all-or-none cell fate responses are incompletely understood. In the *Drosophila* ovary, high and sustained levels of the secreted morphogen Unpaired (Upd) specify the migratory border cell population by activating the Signal Transducer and Activator of Transcription (STAT)[1,2]. Lower and transient STAT activity specifies a non-migratory population of follicle cells[3,4]. Here we identify miR-279 as a component of a feedback pathway that further dampens the response in cells with low JAK/STAT activity. miR-279 directly repressed STAT, whereas loss of miR-279 mimicked STAT gain-of-function or loss of Apontic (Apt), a known feedback inhibitor of STAT. Apt was essential for miR-279 expression in non-migratory follicle cells whereas another STAT target, Ken and Barbie (Ken), down-regulated miR-279 in border cells. Mathematical modeling and simulations of this regulatory circuit including miR-279, Apt, and Ken supported key roles for miR-279 and Apt in generating threshold responses to the Upd gradient.

Morphogens emanate from a localized source, generate a gradient, and pattern gene expression during development. Target gene responses are not necessarily graded. In fact normal pattern formation frequently requires target gene expression to differ dramatically between neighboring cells, even if there is only a small morphogen concentration difference. Known mechanisms that convert graded signals to all-or-none responses include cooperative binding of Bicoid to the *hunchback* enhancer[5], as well as positive transcriptional feedback[6, 7] and mutual repression of target genes[8].

In the *Drosophila* ovary, STAT functions as a morphogen that patterns follicle cell fates[3]. Fruit fly ovaries are composed of egg chambers, each of which produces an egg. Egg chambers contain 16 germline cells (15 nurse cells and 1 oocyte) enveloped by a monolayer

*To whom correspondence should be addressed to D.J.M., dmontell@jhmi.edu.

Author contributions

W.H.Y. planned the experimental design, conducted the experiments and analyzed data. H. M developed and tested the mathematical model. D.J.M. conceived of the project, participated in experimental design, discussions of results and interpretations, and wrote the manuscript.

of epithelial follicle cells. At each egg chamber pole, a pair of polar cells develops and secretes Upd, a cytokine. Upd diffuses to form an extracellular gradient[9] and specifies distinct cell fates at different concentrations[3, 4]. Border cells differentiate immediately adjacent to the anterior polar cell pair, where the morphogen concentration is highest. STAT activity is indispensable for the specification and migration of border cells[1, 10]. Although initially Upd activates STAT in a gradient across ~12 cells, only 4–6 cells differentiate as migratory border cells and retain high levels of STAT activity, due to a negative feedback circuit that includes the Apontic (Apt) protein[4]. In contrast to graded STAT activity, Apt is expressed relatively uniformly in anterior follicle cells. Those cells in which STAT activity exceeds Apt maintain high STAT, differentiate as border cells, invade the neighboring nurse cells and migrate, carrying the polar cells with them[4]. Cells in which Apt inhibition exceeds STAT activation, differentiate as squamous follicle cells and remain within the epithelium[4]. It is unclear however by what molecular mechanism Apt antagonizes STAT.

We investigated the possibility that one or more microRNAs (miRNAs) might function in patterning follicle cell fates and STAT activity. MiRNAs are non-coding 22–24 nucleotide RNAs that repress gene expression post-transcriptionally by partial pairing with the 3' UTR of specific mRNAs[11]. MiRNAs can fine-tune target gene expression levels[12]. To test whether a miRNA might modulate morphogen gradient responses, we searched for miRNAs predicted to bind the 3'UTRs of core genes in the JAK/STAT pathway. We used the following target prediction programs - miRanda[13], PicTar[14], and TargetScan[15], as well as a database[16]. Of the four components – *Upd*, *Domeless* (*Dome*), *Hopscotch* (*hop*), and *STAT92E* examined, only *STAT92E* and *UPD* 3'UTRs contain putative miRNA binding sites. The miRNAs predicted to bind the *STAT* 3'UTR were *miR-279*, *miR-277*, *miR-280*; *miR-284*, *miR-92a*; in addition, the *Upd* 3' UTR contained one predicted *miR-279* binding site. The candidate miRNAs were then overexpressed in S2 cells. Only *miR-279* repressed expression of a reporter gene fused to the *STAT* 3'UTR (Fig. 1a). Overexpression of *miR-279* did not repress expression of a mutant *STAT* 3'UTR reporter gene lacking the *miR-279* seed-binding site (Fig. 1b, c). Furthermore, knock-down of endogenous *miR-279* using a 2'-O-methyl miR-279 antagomir increased *STAT* 3'UTR reporter activity in S2 cells, whereas control antagomirs did not (Fig. 1d). Thus, *miR-279* directly targeted *STAT* via its 3'UTR. Although the *Upd* 3'UTR contained one putative *miR-279* site, the *Upd* 3'UTR reporter did not respond to *miR-279* overexpression (Fig. 1e). Thus, *miR-279* targets the JAK/STAT signaling pathway by repressing STAT.

To determine whether *miR-279* was expressed in the *Drosophila* egg chamber, we examined transgenic flies containing a transcriptional reporter *miR-279-Gal4* and *UAS-GFP*[17]. We detected expression in most follicle cells beginning at stage 8 (Fig. 1f–i). However, *miR-279* expression was undetectable in polar cells (Fig. 1g, i, k, m) and was somewhat lower and more variable in border cells than in non-migratory anterior follicle cells (Fig. 1f–u).

If *miR-279* normally inhibited JAK/STAT signaling, loss-of-function of *miR-279* might cause phenotypes similar to gain-of-function of STAT. Consistent with this hypothesis, extra cells invaded in between the nurse cells in egg chambers containing *miR-279* mutant clones (Fig. 2b), compared to controls (Fig. 2a), a phenotype also observed following ectopic activation of STAT[1,4,10]. We then expressed a *miR-279* "sponge" (an RNA containing 3

copies of the *miR-279* binding site) using *miR-279-Gal4*, as an alternative method to reduce *miR-279* function[18, 19]. This treatment also resulted in ectopic invasive cells (Fig. 2c). Ectopic cells or clusters were observed in approximately 50% of egg chambers following the induction of clones using three different *miR-279* alleles, a phenotype that was ameliorated by the addition of a wild-type *miR-279* transgene to the genetic background (Fig. 2g). Ectopic cells or clusters were also observed in 30% of egg chambers expressing two copies of the *miR-279* sponge (Fig. 2h). To determine whether the abnormal cells came from dissociation of the original border cell cluster or from abnormal invasion of follicle cells that normally remain within the epithelium, we counted the number of cells in the main cell cluster, which contains the polar cells. In all *miR-279* mutant clones, we found that the number of border cells within the main cluster was normal (Fig. 2i).

The level of STAT protein expression in border cells is critical. In fact, in *stat/+* heterozygous females border cells fail to complete their migration by stage 10 in 10% of egg chambers[1,10]. This is highly unusual as most mutations that affect border cells are fully recessive. Over-expression of STAT also impaired border cell migration (Fig. 2d, j), as does STAT hyperactivation[1]. Similarly, mutation of *miR-279* caused frequent border cell migration defects (Fig. 2e), in contrast to wild-type (Fig. 2a). Approximately 50% of border cells mutant for any one of the three alleles, failed to migrate normally, a phenotype that was rescued by the wild-type *miR-279* transgene (Fig. 2k). Knock down of *miR-279* function by expressing the *miR-279* sponge in border cells using *slbo-Gal4* similarly resulted in migration defects (Fig. 2f, l). Together these results show that loss of *miR-279* mimics both phenotypes associated with STAT gain-of- function[1,4,10].

To confirm that *STAT* is a target of *miR-279 in vivo*, we assessed nuclear STAT protein levels using an antibody. STAT was enriched ~1.6 fold in *miR-279* mutant border cells compared to adjacent wild-type cells in mosaic clusters (Fig. 3a; Supplementary information, Fig. S1). In addition, we measured STAT activity using a reporter construct containing 10 STAT binding sites upstream of GFP (10XSTAT92E-GFP)[20]. In wild-type stage 10 egg chambers, STAT activity is predominantly localized in border cells (Fig. 3b, c; Supplementary information, Movie S1). Reducing *miR-279* function using the *miR-279-Gal4* driver to express the *miR-279* sponge, dramatically elevated STAT activity in other follicle cells (Fig. 3d, e; Supplementary information, Movie S2), consistent with the relatively high level of miR-279 Gal4 expression in those cells. Taken together, these results demonstrated that *miR-279* repressed STAT protein expression and activity *in vivo*.

To determine the functional significance of STAT as a *miR-279* target, we tested for genetic interactions. If the *miR-279* phenotypes were primarily caused by excess STAT expression, reducing the level of STAT might ameliorate them. Remarkably, reducing STAT expression using a homozygous hypomorphic, P-element insertion allele ($stat^{ep3391}$) rescued the ectopic invasive cell phenotype (Fig. 3f) and the border cell migration defect in *miR-279* mutant clones (Fig. 3g) to a similar extent as the wild-type *miR-279* transgene. Reducing STAT expression with $stat^{ep3391}$/+ suppressed the *miR-279* sponge phenotype (Fig. 3h). Overexpression of *miR-279* also rescued border cell migration defects caused by overexpression of a *STAT* cDNA, which contained both the protein coding sequence and the normal 3‘UTR (Fig. 3i). Whereas only 30% of border cells over-expressing STAT

completed migration normally, nearly 80% of border cells over-expressing STAT together with *miR-279* completed migration. In contrast, over-expression of *miR-279* did not rescue the phenotype caused by over-expression of STAT with a mutated 3'UTR in which the *miR-279* seed sequence was deleted. In the presence or absence of *miR-279*, approximately 40% of clusters completed migration normally (Fig. 3i). Taken together, these results indicate that STAT is a functional target of *miR-279 in vivo*.

A genetic regulatory circuit consisting of STAT, Apt, and Slow Border Cells (SLBO) was previously shown to convert the initially graded Upd/JAK/STAT signal into "on-off" states of STAT activation[4,21]. Therefore, we decided to investigate how *miR-279* was related to the other components of the circuit. Apt functions as a feedback repressor of STAT whereas SLBO amplifies STAT activity by antagonizing Apt function[4,21]. However, the mechanism by which Apt negatively regulates STAT is unknown.

Since *miR-279* causes phenotypes very similar to *apt*, and Apt is a nuclear protein in follicle cells, we tested whether Apt affects *miR-279* expression. In striking contrast to wild-type (Fig. 4a, b), *miR-279* expression was undetectable in *apt* mutant egg chambers (apt^{167}/ $apt^{KG05830}$) (Fig. 4c, d). We confirmed this result using a *miR-279* activity sensor, which expresses GFP under the control of the tubulin promoter and contains six *miR-279* binding sites in the 3'UTR, rendering GFP expression sensitive to *miR-279*. Consistent with loss of *miR-279* expression in *apt* mutant egg chambers, expression of the sensor was elevated in (apt^{167}/ $apt^{KG05830}$) compared to the wild-type control (Supplementary information, Fig. S2a). A control "sensor" which lacked the critical miR-279 seed sequence showed no difference between wild-type and the *apt* mutant. (Supplementary information, Fig. S2b). Therefore, Apt is essential for *miR-279* expression and activity in follicle cells.

Genetic interactions between *apt* and *miR-279* were consistent with the observation that *miR-279* expression was undetectable in *apt* mutant egg chambers. Knock-down of *miR-279* enhanced the extra invasive cell phenotype in females heterozygous for an *apt* null allele (apt^{167}/+) (Fig. 4e), but did not enhance the extra invasive cell phenotype in homozygous mutants (apt^{167}/ $apt^{KG05830}$) (Fig. 4e). 75–80% of apt^{167}/ $apt^{KG05830}$ mutant egg chambers contain extra invasive cells[4] (Fig. 4e) compared to 45–50% of *miR-279* mutants (Fig. 2g), and STAT expression is elevated three-fold in *apt* mutant border cells[4] compared to 1.6-fold for *miR-279* (Fig. 3a). Therefore, although there are likely additional Apt targets, *miR-279* is an important one in repressing STAT activity and anterior follicle cell invasion.

Apt is expressed in most follicle cells up to stage 8[4]. During stage 9, Apt is expressed across the anterior field of follicle cells in a broad and shallow gradient (Fig. 4g). However unlike Apt, *miR-279* is repressed in cells immediately adjacent to the polar cells, which become border cells (Fig. 4a, b). Therefore we wondered which gene(s) might repress *miR-279* in border cells. *Ken & Barbie (Ken)* is the *Drosophila* homologue of human BCL6, a BTB/POZ domain-containing transcriptional repressor[22]. Ken expression is border cell-enriched based on a microarray analysis and *in situ* hybridization[23], which we confirmed using a *ken* enhancer trap insertion[24, 25] (Fig. 4h, i). To test the effect of Ken on *miR-279* expression, we crossed the *miR-279* reporter into the ken^{k11035}/ ken^{1} mutant background. In wild-type egg chambers, *miR-279-Gal4* expression in border cells was about half of that of

anterior non-migratory border cells, whereas in ken^{k11035}/ken^{1} mutants, the ratio was close to 1 (Fig. 4j). Over-expression of Ken also decreased *mir-279* promoter activity in S2 cells (Supplementary information, Fig. S3). In a microarray analysis, Ken mRNA was significantly upregulated in response to over-expression of Upd in follicle cells (Wang, X. and Montell, D. J., unpublished data), which is also true in eye imaginal discs[26]. Ken expression is also highest in border cells (Fig. 4h, i), where STAT activity is highest, suggesting *ken* could be a STAT target. Consistent with this inference, in egg chambers mutant for a temperature-sensitive *stat* allele ($stat^{397}/stat^{ts}$) incubated at the restrictive temperature, Ken expression was reduced in border cells (but not polar cells which have little or no active STAT) compared to control (Fig. 4k–o). Therefore in border cells, *ken* is a target of STAT.

Together these data suggest a model for the conversion of the graded Upd signal into migratory border cell and stationary epithelial cell fates (Fig. 5a,b). We previously developed a mathematical model and used simulations of the patterning process to show that a gene regulatory circuit consisting of STAT, Apt, and Slbo was sufficient[4]. However, it was unclear how Apt exerted its effect on STAT. The results presented here suggest that *miR-279* is a major target of Apt that directly targets STAT (Fig. 5a, b). We used a set of differential equations to approximate the relative concentration of each component across the field of the epithelium in computer simulations (see methods). Multiple iterations of these computations led to evolving patterns of gene expression, which accurately reproduced the observed patterns of *miR-279*, STAT, Apt, Ken, and Slbo over time (Fig. 5c–f). In the simulations loss of *miR-279*, like loss of *apt*, resulted in failure of the proper pattern of JAK/STAT activity to form (Fig. 5g, h). We note that the deterministic (rather than probabilistic) nature of the model does not permit simulation of incomplete penetrance and thus does not reproduce the difference in penetrance between these two (80% for *apt* vs. 50% for *miR-279*).

Interestingly, in simulations, loss of *ken* still permitted development of “on” and “off” states (Fig. 5i). Experimentally, we also found that loss of *ken* in mosaic clone analyses did not impede border cell migration, and forced expression of UAS-*miR-279* with *slbo-Gal4>UAS-miR-279* was similarly benign (not shown). The simulations show that the mutual repression between Slbo and Apt is sufficient to ensure relatively robust patterning, even in the absence of *ken*. The modeling and genetic results both show that this regulatory circuit is more sensitive to loss than gain of *miR-279*.

Complex genetic networks are required for a variety of biological phenomena, however their complexity often challenges our intuitive understanding. Mathematical modeling can be useful for probing the behavior of such complex systems[27]. Here the mathematical model revealed non-obvious features of the morphogen interpretation system. One interesting feature of this system is that non-linear positive auto-regulation of the JAK/STAT pathway is not responsible for creating the threshold response of target gene expression. Even though such auto-regulation can produce threshold responses, and auto-regulation is a property of JAK/STAT signaling, by itself it does not produce the initially graded pattern observed here. The multiple positive and negative feedback loops shown here can produce a more complex

response, including a transient response to a low level of morphogen, which is not characteristic of a response dominated by non-linear auto-regulation.

In this work we describe a key role for *miR-279* in shaping threshold responses to the Upd morphogen gradient. Apt-mediated expression of *miR-279* is critical to repress STAT in anterior follicle cells destined to remain within the epithelium. Since *miR-279* provides post-transcriptional control of STAT, it can repress the function of pre-existing mRNA and in principle lead to a swifter and more decisive cellular response than feedback at the level of transcription alone. Thus miRNA-mediated feedback may be particularly important in tissues undergoing rapid development. In addition, this mechanism creates not only a lower level response but also a transient response. In some morphogen systems, the length of time that a cell experiences the signal is important for generating correct cell fates[27]. Border cells represent such a system. Border cells that express a temperature-sensitive form of STAT and are shifted to the non-permissive temperature part way through their migration, turn on expression of at least one anterior follicle cell marker after 2.5 hours. Therefore a transient STAT signal may specify anterior cell fate even if it first reaches a level high enough to promote border cell fate and migration[10]. *miR-279* is part of the mechanism that terminates STAT signaling and thus specifies anterior follicle cell fate. Another tissue in which sustained versus transient STAT signaling is important is in stem cell fate specification in the Drosophila testis. It will be of interest to determine if *miR-279* also contributes to patterning fates in this context as well.

Methods

Fly strains and fly genetics

mir-279$^{\Delta 1.2}$, *mir-279*$^{\Delta 1.9}$, *FRT82B mir-279*^{S096207}, *mir-279-GAL4*, and flies bearing the *mir-279* genomic transgene were generously provided by the lab of S. Lawrence Zipursky[17]. *FRT82B mir-279*$^{\Delta 1.2}$, *FRT82B mir-279*$^{\Delta 1.9}$, and *FRT82B mir-279*^{S096207}, *stat*^{ep3391} were generated by recombination for this study. *stat* lines used were: *stat*^{397} (ref.1), *stat*^{ep3391} (ref.10), *stat*^{ts} (a gift of Charles Dearolf)[28], and *UAS-STAT*[29]. *apt*^{167} was obtained from W. McGinnis[30]. *Ken*^{k11035} was a gift from M. P. Zeidler[22]. 10XSTAT92E-GFP was a gift from N. Perrimon[20]. Other *Drosophila* lines were obtained from the Bloomington Stock Center: P{SUPor-P}*apt*^{KG05830}, P{PZ}*ken*^{1}, and P{PZ}*ken*^{02970}.

Mosaic analysis was performed as follows: mutations on *FRT82B* chromosomes were crossed to *hsFLP; FRT82B UbiGFP*^{nls} flies. Flies with the *hsFLP/+; FRT82B miR-279 mutant allele* (e.g. *mir-279*$^{\Delta 1.2}$) */FRT82B UbiGFP*^{nls} genotype were heat shocked for 1 hour three times a day for 2–3 consecutive days, then dissected 7–10 days later. Mutant clones were marked by the loss of GFP. As a control, flies with the *hsFPL/+; FRT82B/FRT82B UbiGFP*^{nls} genotype were used. Alternatively, the MARCM technique was used to label homozygous mutant cells with GFP, as previously described[31]. Female flies with the genotype *P[hsp70-flp], UAS-mCD8GFP/c306-GAL4; FRT82B GAL80/FRT82B miR-279 mutant allele* (e.g. *mir-279*$^{\Delta 1.2}$) were heat shocked as described above. GAL4 drivers used include *slbo-Gal4* (ref.32), *c306-GAL4* (ref.33), and *miR-279-GAL4*. These were crossed with UAS transgenes[34] at 25°C. Progeny were incubated on fresh food with yeast paste overnight at 31°C prior to ovary dissection. All crosses with *stat*^{ts} were carried out at the

permissive temperature (18°C), then shifted to non-permissive temperature (29°C) overnight prior to ovary dissection.

Immunohistochemistry and Imaging

Ovaries were dissected in S2 medium (Invitrogen) containing 10% fetal bovine serum, fixed in 4% formaldehyde for 10 minutes at room temperature, and then rinsed three times in phosphate buffered saline with 0.3% Triton X-100. The following primary antibodies from the Developmental Studies Hybridoma Bank (DSHB) were used for immunostaining: mouse anti-Armadillo (1:25), mouse anti-EYA (1:25), mouse anti-Fascillin III (1:10), and mouse anti-β-galactosidase (1:10). Other primary antibodies used were: Rabbit anti-GFP (1:2,000; Molecular Probes), rabbit anti-STAT (1:1,000)[4], and rabbit anti-Apontic (1:2,000; a gift of Reinhard Schuh)[35]. Secondary antibodies conjugated to Alexa-488, Alex-568 were used at 1:400 dilutions (Molecular Probes). The images were obtained using a Zeiss LSM 510-Meta confocal microscope or the ApoTome system on a Zeiss Axioplan 2 microscope. To quantify nuclear protein levels (e.g. STAT, Apt, and LacZ), pixel intensity of each protein was normalized to pixel intensity of DAPI in equivalent regions. To calculate the ratio of nuclear STAT level in *miR-279* mutant border cells to that in wild-type border cells, the average of normalized nuclear STAT levels in *miR-279* mutant clones or *FRT82B* clones (control) was divided by the average of normalized nuclear STAT levels in wild-type cells in the same cluster. Pixel intensities of images were quantified using Image J. Statistical significance of differences was assessed using a student t-test. For confocal micrographs of egg chambers expressing the *miR-279* sensor or control sensor, we captured all images using identical exposure time, laser gain, and offset.

Transgenic constructs

The *UAS-miR-279* construct was generated by cloning a 614 bp fragment, centered around the *miR-279* stem-loop precursor, downstream of *pUASpDsRed*. PCR primers for *miR-279* were 5'-GGATCCTGTGTAGAGCTGATAAGAAG-3' and 5'-TCTAGAGCATTAATTTTCATTTTATTTCGG-3'.

The miR-279 sponge construct was cloned as follows: We phosphorylated, annealed, and cloned 87 bp oligonucleotides containing 3 copies of perfect mir-279 binding site into the 3'UTR of *pUASpDsRed*. The oligonucleotide sequences were used for miR-279 sponge: miR-279 sponge–F 5'-GATCCATAGCTTAATGAGTGTGGATCTAGTCAGGCTAGCCTTAATGAGTGTGGATCTAGTCACCACAGTGTTAATGAGTGTGGATCTAGTCAT-3'

miR-279 sponge –R: 5'-TAGATGACTAGATCCACACTCATTAACACTGTGGTGACTAGATCCACACTCATTAAGGCTAGCCTGACTAGATCCACACTCATTAAGCT ATG-3'

The miR-279 binding sites are underlined.

For construction of *UAS-STAT wt 3'UTR*, the *STAT* coding sequence and its *3'UTR* were amplified by PCR from wild-type ovary cDNA and cloned into *pUAST* construct. PCR

primers used were 5’-GAATTCATGAGCTTGTGGAAGCGC-3’ and 5’-GCGGCCGCCAAACGTAATATGGTCCTCG-3’.

UAS-STAT mut 3’UTR was generated by deletion of *miR-279* seed binding site in *STAT* 3’UTR using the QuickChange Site-Directed Mutagenesis kit (Stratagene). The primers used for site-directed mutagenesis of *miR-279* seed sequence in *STAT* 3’UTR were: 5’-CGCCACATGCGATTGCCTTGCTATTAGAGACACGAGGACC-3’ and 5’-GGTCCTCGTGTCTCTAATAGCAAGGCAATCGCATGTGGCG-3’.

For construction of *miR-279* sensor, 161 bp oligonucleotides containing 6 copies of *miR-279* binding sites of *STAT 3’UTR* were cloned into 3’UTR of pCaSpeR-tub-GFP-bam 3’UTR (a gift from Toshie Kai)[36] after deletion of bam 3’UTR from the vector.

The oligonucleotide sequences were used for miR-279 sensor: miR-279 sensor -F: 5’-GGCCGcaCATGCGATTGCCTTTTTAGTCAgccaCATGCGATTGCCTTTTTAGTCAgccaCATGCGATTGCCTTTTTAGTCAgccaCATGCGATTGCCTTTTTAGTCAgccaCATGCGATTGCCTTTTTAGTCAgccaCATGCGATT GCCTTTTTAGTCAgc-3’

miR-279 sensor -R: 5’-TCGAgcTGACTAAAAAGGCAATCGCATGtggcTGACTAAAAAGGCAATCGCATGtggcTGACTAAAAAGGCAATCGCATGtggcTGACTAAAAAGGCAATCGCATGtggcTGACTAA AAAGGCAATCGCATGtgC-3’

Control sensor was generated in the same way as the *miR-279* sensor using 119 bp oligonucleotides in which all six miR-279 seed binding sites were deleted. The oligonucleotide sequences used were: Control sensor -F: 5’-GGCCGcaCATGCGATTGCCTTAgccaCATGCGATTGCCTTAgccaCATGCGATTGCCTTAgccaCATGCGATTGCCTTAgccaCATGCGATTGCCTTA gccaCATGCGATTGCCTTAgc-3’

Control sensor -R: 5’-TCGAgcTAAGGCAATCGCATGtggcTAAGGCAATCGCATGtggcTAAGGCAATCGCATGtggcTAAGGCAATCGCATGtggcTAAGGCAATCGCATGtggcTAAGGCAATCGCATGtgC-3’

Cloned constructs were microinjected into *w1118* embryos, and multiple transgenic lines were established.

miRNA target prediction

We made a list of potential *STAT* 3’UTR-binding miRNAs, including miRNA family members sharing the same seed sequence (such as *miR-279* and *miR-286*) from available target prediction programs (miRanda[13], PicTar[14], and TargetScan[15]) and a dataset available at HYPERLINK " HYPERLINK "http://cbio.mskcc.org/research/sander/data/miRNA2003/drosophila/index.html" " HYPERLINK "http://cbio.mskcc.org/research/sander/data/miRNA2003/drosophila/index.html"[16]

Luciferase reporter assays

For validation of miRNAs that target *STAT* 3'UTR, a 418 bp fragment of the *STAT* 3'UTR was amplified by PCR from wild-type genomic DNA and cloned downstream of Renilla luciferase in the psiCheck-2 vector (Promega). PCR primers for amplification of the *STAT* 3'UTR: 5'-CTCGAGTTTAATTCGCGTGCTAAGCC-3' and 5'-GCGGCCGCGGGGTGTACTTAAGTCTTATAAAA-3'. The predicted *miR-279* target site in *STAT* 3'UTR was mutated using the same oligonucleotides used for construction of *UAST* STAT mut 3'UTR as described above.

Primer sets used for cloning of other miRNAs were:

miR-92a-Forward: 5'-GGATCCTCAAGTAGGGGCGGAAATTTAATA-3

miR-92a-Reverse: 5'-TCTAGATATCAAATGTAACTGGGAAGTGTG-3

miR-277- Forward: 5'-CTTTGGAGTTGCACCTTCGATTTC-3

miR-277- Reverse: 5'-CTTGGCAGAAAAAGTAGAATAAAAC-3

miR-280- Forward: 5'-GGATCCATGGACATGTGTGTGTGTGC-3

miR-280- Reverse: 5'-TCTAGATTAGTTCTAATCATTTTATATGCC-3

miR-284- Forward: 5'- GGATCCATATAGTGCATCGATATCAG-3' miR-284-Reverse: 5'-TCTAGAAATCGGTAAGTTTTGCAAAC-3'

PCR fragments containing miRNA precursors were cloned downstream of *pUASp-DsRed*. For *miR-279* promoter reporter gene assay, a 1945 bp fragment of the *miR-279* promoter region was amplified by PCR from wild-type genomic DNA, and cloned upstream of firefly luciferase in pGL3 basic (Promega). PCR primers used for *miR-279* promoter were:

miR-279 promoter-F: 5'-GCTAGCTGAAAATACGCGTATGGAAATGCC-3'

miR-279 promoter-R: 5'-CTCGAGCAGCTCCAGTCCCAATTCC-3'

3' UTR reporter assay was performed as follows. a combination of 100 ng *STAT* 3'UTR reporter, 50 ng *Act5C-GAL4* and 300 ng *UAS-DsRed-miRNA* or *miRNA sponge* constructs was transfected in duplicate into 1×10^6 S2 cells in 12 well plates. *miR-279* promoter reporter gene assay was performed as follows. A combination of 100 ng *miR-279* promoter reporter, 50ng *pAct-Renilla*, 50 ng *Act5C-GAL4*, and 300 ng *pUAST-Ken* (a gift of M. P. Zeidler)[22] constructs was transfected in duplicate into 1×10^6 S2 cells in 12 well plates. Two days after transfection, the cells were lysed in passive lysis buffer, and dual luciferase assay was carried out (Promega), and analyzed on a luminometer.

For the 2'-O-methyl antagomir mediated de-silencing assay, a combination of *STAT 3'UTR* reporter (100 ng), and 10pmol (100nM) of 2'-O-methyl antagomir (2'Ome miR-279: TTAATGAGTGTGGATCTAGTCA; 2'Ome miR-280: TATCATTTCATATGCAACGTAAATACA; 2'Ome miR-iab-4-3p: GTTACGTATACTGAAGGTATACCG) (Dharmaco RNAi Technologies & Integrated DNA Technologies) was transfected in duplicate into 1×10^6 S2 cells in 12 well plates. Three

days after transfection, the cells were lysed in passive lysis buffer, and dual luciferase assays were carried out (Promega), and analyzed on the luminometer.

Relative luciferase activity was obtained by calculating the ratio of Renilla luciferase activity to a firefly luciferase control in 3'UTR reporter assay. Relative luciferase activity indicates the ratio of firefly luciferase activity to a Renilla luciferase control in *miR-279* promoter reporter assay.

Mathematical model and computer simulation

In comparison with the earlier model[4], the work described in this paper suggested the following modifications: *miR-279* (*R*) is produced under the control of Apt, its synthesis is inhibited by Ken, and *miR-279* has an inhibitory influence on JAK/STAT. SLBO is assumed to has an inhibitory influence not only on the production of Apt but also undermines the inhibition of *miR-279* on the production rate JAK/STAT (Fig. 6a, b). The model works in the following way: *miR-279*, produced under JAK/STAT-control via Apt, eventually down-regulates JAK/STAT. Only at high JAK/STAT levels is sufficient SLBO produced that abolishes this JAK/STAT down-regulation, leaving a high JAK/STAT level as required for border cell formation. The all-or nothing behaviour is based on the nonlinearities in the interactions.

The following set of partial differential equations describes the concentration change per time unit of JAK/STAT *(J)*, UDP *(U)*, Apt *(A)*, SLBO *(S)*, *miR-279 (R)* and Ken *(K)*. Since the actual parameters are unknown, parameters have been chosen such that the observed concentration profiles of the wild-type and of the mutants are reproduced (Supplementary information, Table 1). For the simulation, these equations are re-written as difference equations. Initially, all concentrations are assumed to be zero except of a polar cell activator *P*, whose concentration remains unchanged. The equations allow computing the concentration change in a small time interval. Adding these changes to the existing concentrations leads to the new concentrations. Repeating such computations leads to the total time course. After ca. 50000 such iterations a stable steady state is reached (corresponding to ca. 360 min of real development).

$$\frac{\partial J}{\partial t}=\frac{p_j\,U}{(1+q_j\,P^2+a_j\,R/(1+k_j\,S^2)}-r_j\,J \quad \text{(Eq. 1)}$$

$$\frac{\partial U}{\partial t}=p_u\,P-r_u\,U+D_u\frac{\partial^2 U}{\partial x^2} \quad \text{(Eq. 2)}$$

$$\frac{\partial A}{\partial t}=\frac{p_a\,J}{1+q_a S}-r_a\,A+b_a \quad \text{(Eq. 3)}$$

$$\frac{\partial S}{\partial t}=\frac{p_s\,J^2}{1+q_s{}^A}-r_s\,S \quad \text{(Eq. 4)}$$

$$\frac{\partial R}{\partial t} = \frac{p_r A}{1 + q_r K^2} - r_r R \quad \text{(Eq. 5)}$$

$$\frac{\partial K}{\partial t} = p_k J - r_k K \quad \text{(Eq. 6)}$$

For the function of the system it is important that the inhibition of JAK/SLBO by *miR-279* is linear ($a_j R$ in Equation 1) but that the undermining of this inhibition by SLBO is non-linear ($k_j S^2$ in Equation 1). This has the consequence that only at high JAK/STAT and thus at high SLBO levels the JAK/STAT production is protected from the *miR-279* inhibition, allowing the maintenance of high JAK/STAT levels there. The system is fairly robust to changes in the parameters; examples for this and further details are given in the Supplementary Information.

Supplementary Material

Refer to Web version on PubMed Central for supplementary material.

Acknowledgements

This work was supported by NIH grant GM46425 to D.J.M. W.H.Y. was supported by a fellowship from the Korea Science and Engineering Foundation (KOSEF) and the H.A. and Mary K. Chapman Young Investigator Fellowship. We acknowledge Amanda H. McDonald and Brandon Steiner for technical assistance. We thank Jae Sun Kang for data illustration. We thank Melanie Issigonis for helpful discussion. We thank current and past members of the Denise Montell and Craig Montell labs for helpful discussion and comments. Flybase and the Bloomington Drosophila Stock Center provided critical information and reagents for this study.

References

1. Silver DL, Montell DJ. Paracrine signaling through the JAK/STAT pathway activates invasive behavior of ovarian epithelial cells in Drosophila. Cell. 2001; 107:831–841. [PubMed: 11779460]
2. Ghiglione C, et al. The Drosophila cytokine receptor Domeless controls border cell migration and epithelial polarization during oogenesis. Development. 2002; 129:5437–5447. [PubMed: 12403714]
3. Xi R, McGregor JR, Harrison DA. A gradient of JAK pathway activity patterns the anterior-posterior axis of the follicular epithelium. Dev Cell. 2003; 4:167–177. [PubMed: 12586061]
4. Starz-Gaiano M, Melani M, Wang X, Meinhardt H, Montell DJ. Feedback inhibition of Jak/STAT signaling by apontic is required to limit an invasive cell population. Dev Cell. 2008; 14:726–738. [PubMed: 18477455]
5. Driever W, Nusslein-Volhard C. The bicoid protein determines position in the Drosophila embryo in a concentration-dependent manner. Cell. 1988; 54:95–104. [PubMed: 3383245]
6. Gould A, Morrison A, Sproat G, White RA, Krumlauf R. Positive cross-regulation and enhancer sharing: two mechanisms for specifying overlapping Hox expression patterns. Genes Dev. 1997; 11:900–913. [PubMed: 9106661]
7. Gould A, Itasaki N, Krumlauf R. Initiation of rhombomeric Hoxb4 expression requires induction by somites and a retinoid pathway. Neuron. 1998; 21:39–51. [PubMed: 9697850]
8. Saka Y, Smith JC. A mechanism for the sharp transition of morphogen gradient interpretation in Xenopus. BMC Dev Biol. 2007; 7:47. [PubMed: 17506890]
9. Ghiglione C, Devergne O, Cerezo D, Noselli S. Drosophila RalA is essential for the maintenance of Jak/Stat signalling in ovarian follicles. EMBO Rep. 2008; 9:676–682. [PubMed: 18552769]

10. Silver DL, Geisbrecht ER, Montell DJ. Requirement for JAK/STAT signaling throughout border cell migration in Drosophila. Development. 2005; 132:3483–3492. [PubMed: 16000386]
11. Bartel DP. MicroRNAs: target recognition and regulatory functions. Cell. 2009; 136:215–233. [PubMed: 19167326]
12. Hornstein E, Shomron N. Canalization of development by microRNAs. Nat Genet. 2006; 38(Suppl):S20–S24. [PubMed: 16736020]
13. John B, et al. Human MicroRNA targets. PLoS Biol. 2004; 2:e363. [PubMed: 15502875]
14. Krek A, et al. Combinatorial microRNA target predictions. Nat Genet. 2005; 37:495–500. [PubMed: 15806104]
15. Lewis BP, Burge CB, Bartel DP. Conserved seed pairing, often flanked by adenosines, indicates that thousands of human genes are microRNA targets. Cell. 2005; 120:15–20. [PubMed: 15652477]
16. Enright AJ, et al. MicroRNA targets in Drosophila. Genome Biol. 2003; 5:R1. [PubMed: 14709173]
17. Cayirlioglu P, et al. Hybrid neurons in a microRNA mutant are putative evolutionary intermediates in insect CO2 sensory systems. Science. 2008; 319:1256–1260. [PubMed: 18309086]
18. Ebert MS, Neilson JR, Sharp PA. MicroRNA sponges: competitive inhibitors of small RNAs in mammalian cells. Nat Methods. 2007; 4:721–726. [PubMed: 17694064]
19. Loya CM, Lu CS, Van Vactor D, Fulga TA. Transgenic microRNA inhibition with spatiotemporal specificity in intact organisms. Nat Methods. 2009; 6:897–903. [PubMed: 19915559]
20. Bach EA, et al. GFP reporters detect the activation of the Drosophila JAK/STAT pathway in vivo. Gene Expr Patterns. 2007; 7:323–331. [PubMed: 17008134]
21. Starz-Gaiano M, Melani M, Meinhardt H, Montell D. Interpretation of the UPD/JAK/STAT morphogen gradient in Drosophila follicle cells. Cell Cycle. 2009; 8:2917–2925. [PubMed: 19729999]
22. Arbouzova NI, Bach EA, Zeidler MP. Ken & barbie selectively regulates the expression of a subset of Jak/STAT pathway target genes. Curr Biol. 2006; 16:80–88. [PubMed: 16401426]
23. Wang X, et al. Analysis of cell migration using whole-genome expression profiling of migratory cells in the Drosophila ovary. Dev Cell. 2006; 10:483–495. [PubMed: 16580993]
24. Lukacsovich T, Asztalos Z, Juni N, Awano W, Yamamoto D. The Drosophila melanogaster 60A chromosomal division is extremely dense with functional genes: their sequences, genomic organization, and expression. Genomics. 1999; 57:43–56. [PubMed: 10191082]
25. Castrillon DH, et al. Toward a molecular genetic analysis of spermatogenesis in Drosophila melanogaster: characterization of male-sterile mutants generated by single P element mutagenesis. Genetics. 1993; 135:489–505. [PubMed: 8244010]
26. Flaherty MS, Zavadil J, Ekas LA, Bach EA. Genome-wide expression profiling in the Drosophila eye reveals unexpected repression of notch signaling by the JAK/STAT pathway. Dev Dyn. 2009; 238:2235–2253. [PubMed: 19504457]
27. Schier AF. Nodal morphogens. Cold Spring Harb Perspect Biol. 2009; 1 a003459.
28. Baksa K, Parke T, Dobens LL, Dearolf CR. The Drosophila STAT protein, stat92E, regulates follicle cell differentiation during oogenesis. Dev Biol. 2002; 243:166–175. [PubMed: 11846485]
29. Singh SR, Liu W, Hou SX. The adult Drosophila malpighian tubules are maintained by multipotent stem cells. Cell Stem Cell. 2007; 1:191–203. [PubMed: 18371350]
30. Gellon G, Harding KW, McGinnis N, Martin MM, McGinnis W. A genetic screen for modifiers of Deformed homeotic function identifies novel genes required for head development. Development. 1997; 124:3321–3331. [PubMed: 9310327]
31. Lee T, Luo L. Mosaic analysis with a repressible cell marker for studies of gene function in neuronal morphogenesis. Neuron. 1999; 22:451–461. [PubMed: 10197526]
32. Rorth P, et al. Systematic gain-of-function genetics in Drosophila. Development. 1998; 125:1049–1057. [PubMed: 9463351]
33. Manseau L, et al. GAL4 enhancer traps expressed in the embryo, larval brain, imaginal discs, and ovary of Drosophila. Dev Dyn. 1997; 209:310–322. [PubMed: 9215645]

34. Fischer JA, Giniger E, Maniatis T, Ptashne M. GAL4 activates transcription in Drosophila. Nature. 1988; 332:853–856. [PubMed: 3128741]

35. Eulenberg KG, Schuh R. The tracheae defective gene encodes a bZIP protein that controls tracheal cell movement during Drosophila embryogenesis. EMBO J. 1997; 16:7156–7165. [PubMed: 9384592]

36. Pek JW, Lim AK, Kai T. Drosophila maelstrom ensures proper germline stem cell lineage differentiation by repressing microRNA-7. Dev Cell. 2009; 17:417–424. [PubMed: 19758565]

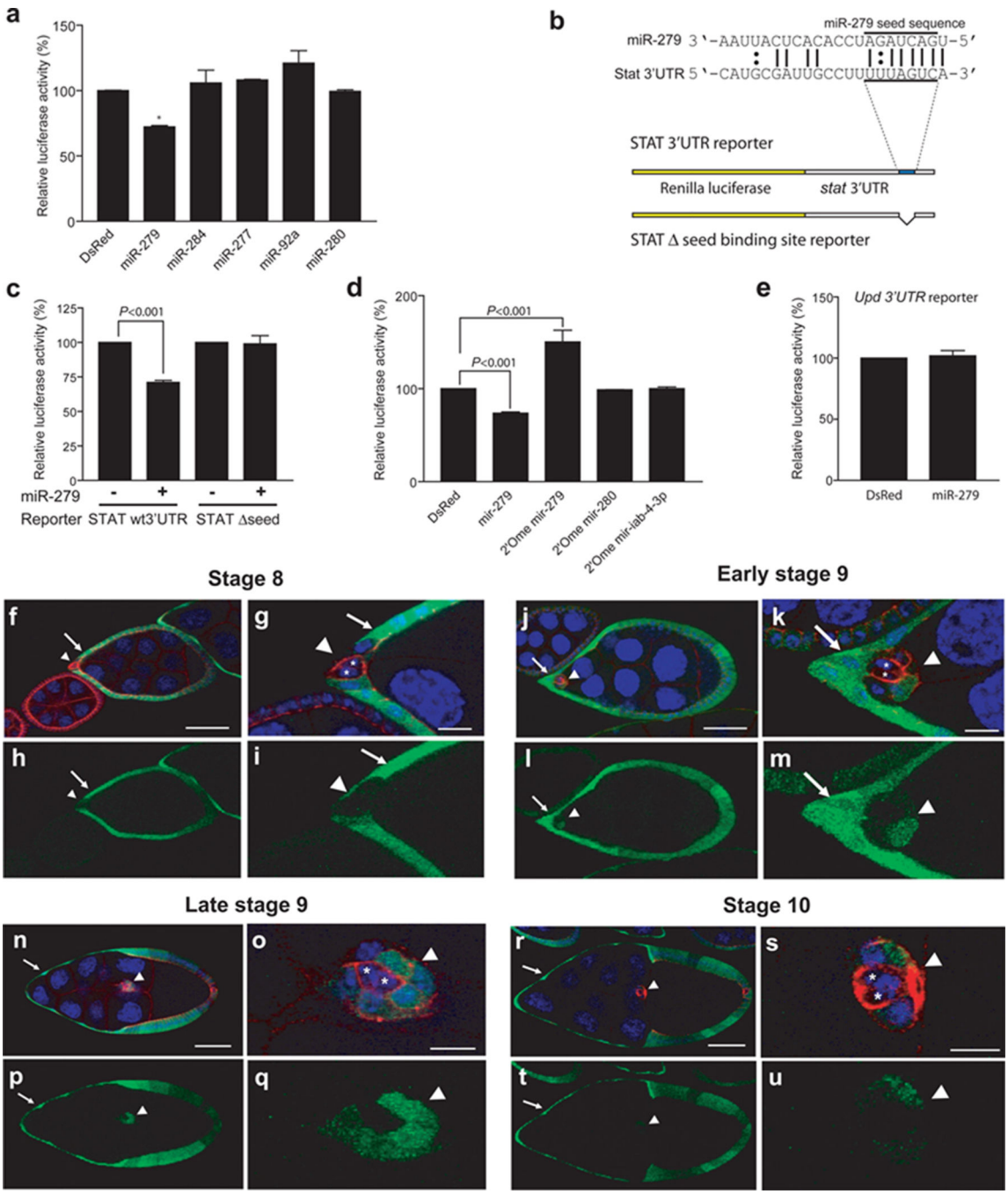

Figure 1. *STAT* is a target of miR-279

(a) Effect of miRNAs on expression of a Renilla luciferase reporter carrying the *STAT* 3'UTR in S2 cells. Error bars indicate SEM. P values were calculated using an ANOVA test. **P*<0.05. Effects of *miR-284*, *miR-277*, *miR-92a* and *miR-280* were not significantly different from the control (*P*>0.3). (b) Schematic representation of *miR-279* pairing with the *STAT* 3'UTR. Lines indicate canonical pairings and double dots indicate non-canonical (G:U) pairings. The seed pairings are underlined. Schematic representation of *STAT* 3'UTR reporter with and without the *miR-279* seed-binding site (blue). Yellow box represents

Renilla luciferase coding sequence and white box represents the 3'UTR. (c) Effect of *miR-279* on expression of a Renilla luciferase reporter carrying the *STAT* 3'UTR with or without the *miR-279* seed-binding sequence. Error bars represent SEMs. P value was calculated using a Student's t test. (d) De-repression of the *STAT* 3'UTR reporter by 2'O-methyl miR-279 antagomir in S2 cells. Error bars represent SEM. P values were calculated using ANOVA. (e) Effect of *miR-279* on expression of a Renilla luciferase reporter carrying the *Upd* 3'UTR in S2 cells. Error bar indicates SEM. Relative luciferase activity is the ratio of Renilla luciferase activity to a firefly luciferase control. (a, c, d, e) (f–u) Confocal micrographs of egg chambers of indicated stages carrying a *miR-279* expression reporter (*miR-279-GAL4; UAS-GFP*)[17]. DAPI (blue) labels nuclei, and Armadillo (red) labels membranes enriched in adherens junction proteins. Arrowheads indicate the border cell cluster, arrows indicate non-migratory anterior epithelial follicle cells, and asterisks indicate polar cells. Scale bars represent 50 μ in f, j, n, and r, and 10 μ in g, k, o and s.

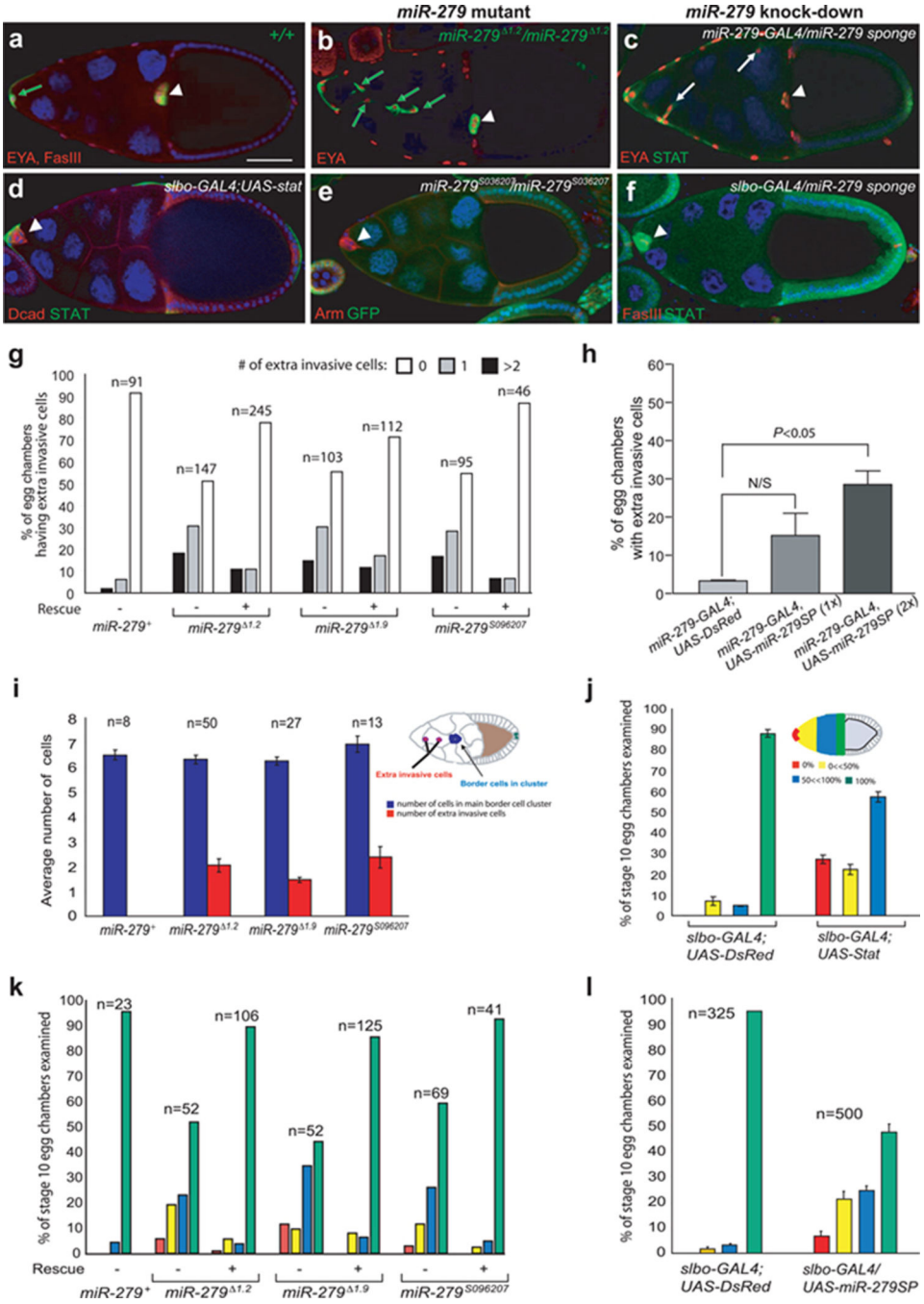

Figure 2. Loss-of-function of miR-279 phenocopies gain-of-function of STAT

(a–f) Confocal micrographs of stage 10 egg chambers of the indicated genotypes. (a, b) MARCM analysis of control (a) and *miR-279* mutant (b) follicle cells. Homozygous mutant cells express GFP (green). Scale bar represents 50 μ. (c) *miR-279* knockdown in follicle cells. Arrows indicate extra invasive cells in b and c. (d) A stage 10 egg chamber in which STAT was overexpressed in border cells using *slbo-GAL4*. (e) Mosaic analysis of the *miR-279*^{S036207} allele. Homozygous mutant cells lack GFP and fail to migrate. (f) *miR-279* knockdown in border cells. Arrowheads indicate border cell cluster (a–f). (g) Quantification

of extra invasive cells in egg chambers mosaic for the indicated *miR-279* alleles in the presence (+) or absence (−) of a transgene containing the wild-type *miR-279* gene. White, gray, and black bars indicate percentage of egg chamber with zero, one, or two or more extra invasive cells, respectively. (h) Effect of *miR-279 sponge* (*miR-279SP*) expression on the percentage of egg chambers containing extra invasive cells. Error bars represent SEM. P values were calculated using a Student's t test. N/S, not significant (i) Effect of the indicated *miR-279* alleles on the number of cells in the border cell cluster (blue) and number of extra invasive cells (red) as depicted in the schematic. Error bards represent SEM. (j) Effect on border cell migration of expressing *UAS-DsRed* or *UAS-STAT* with *slbo-GAL4*. Schematic representation of stage10 egg chamber showing the approach used for quantification of border cell migration. Red shading indicates the region of the egg chamber in which border cells appear when they fail to migrate. Yellow and blue indicate incomplete migration, and green indicates complete migration. (k) Migration of border cell clusters composed entirely of homozygous mutant cells of the indicated *miR-279* alleles in the presence (+) or absence (−) of a transgene containing the wild-type *miR-279* gene. (l) Effect on border cell migration of expressing *UAS-DsRed* or *UAS-miR-279SP* with *slbo-GAL4*.

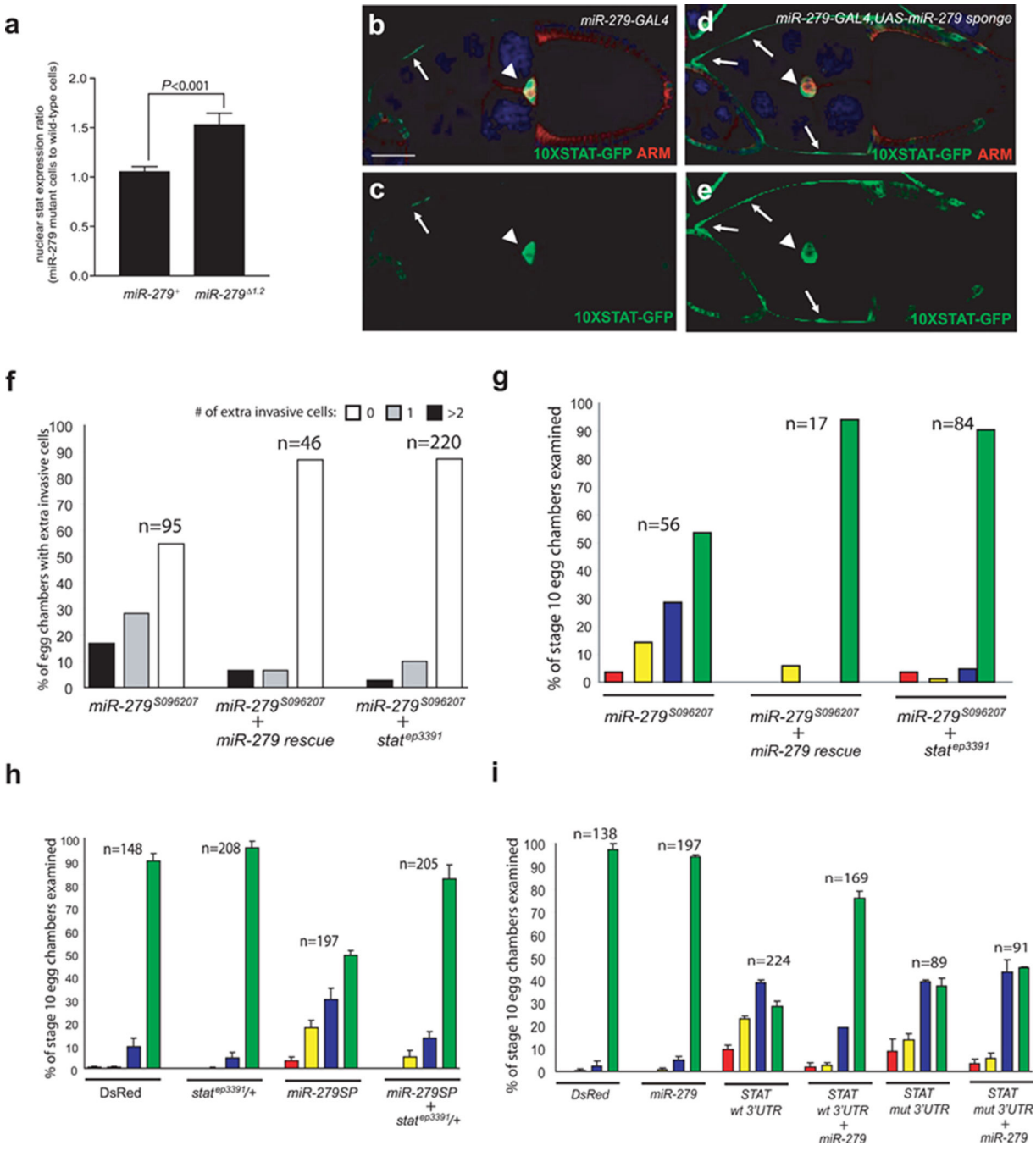

Figure 3. *STAT* is a critical target of miR-279 *in vivo*

(a) Comparison of nuclear STAT levels in wild-type versus homozygous miR-279$^{\otimes 1.2}$ mutant border cells in mosaic clusters (see methods). Error bars represent SEM. P value was calculated using a Student's t test. (b–e) Confocal micrographs of stage 10 egg chambers of the indicated genotypes. GFP expression (green) reflects STAT activity. DAPI (blue) labels nuclei, and Armadillo (red) labels membranes. Arrowheads indicate border cells and arrows indicate non-migratory anterior follicle cells. Scale bars represent 50 μ. (f–i) Genetic interactions between *miR-279* and *stat.* (f) Quantification of egg chambers possessing extra-

invasive cells following induction of *miR-279* mutant clones in the presence of a rescuing transgene or homozygous for a hypomorphic *stat* allele ($stat^{ep3391}$). White, gray, and black bars indicate percentage of egg chamber with zero, one, or two or more extra invasive cells, respectively. (g–i) Quantification of border cell migration defects in stage 10 egg chambers. Red indicates no migration; yellow and blue indicate incomplete migration; green indicates complete migration, as in Figure 3. (g) Egg chambers containing border cell clusters composed entirely of homozygous *miR-279* mutant cells in the presence of a rescuing transgene or homozygous for a hypomorphic *stat* allele ($stat^{ep3391}$). (h) All egg chambers carry *slbo-GAL4*, with or without *UAS-miR-279 sponge* (*miR-279 SP*) and/or $stat^{ep3391}$/+, as indicated. Error bars represent SEMs. (i) All egg chambers carry *slbo-GAL4*, with or without *UAS-miR-279* in combination with *UAS- STAT wt 3'UTR*, which includes both coding and 3'UTR sequences or *UAS- STAT mutant (mut) 3'UTR* in which the *miR-279* seed was deleted. Error bars represent SEMs.

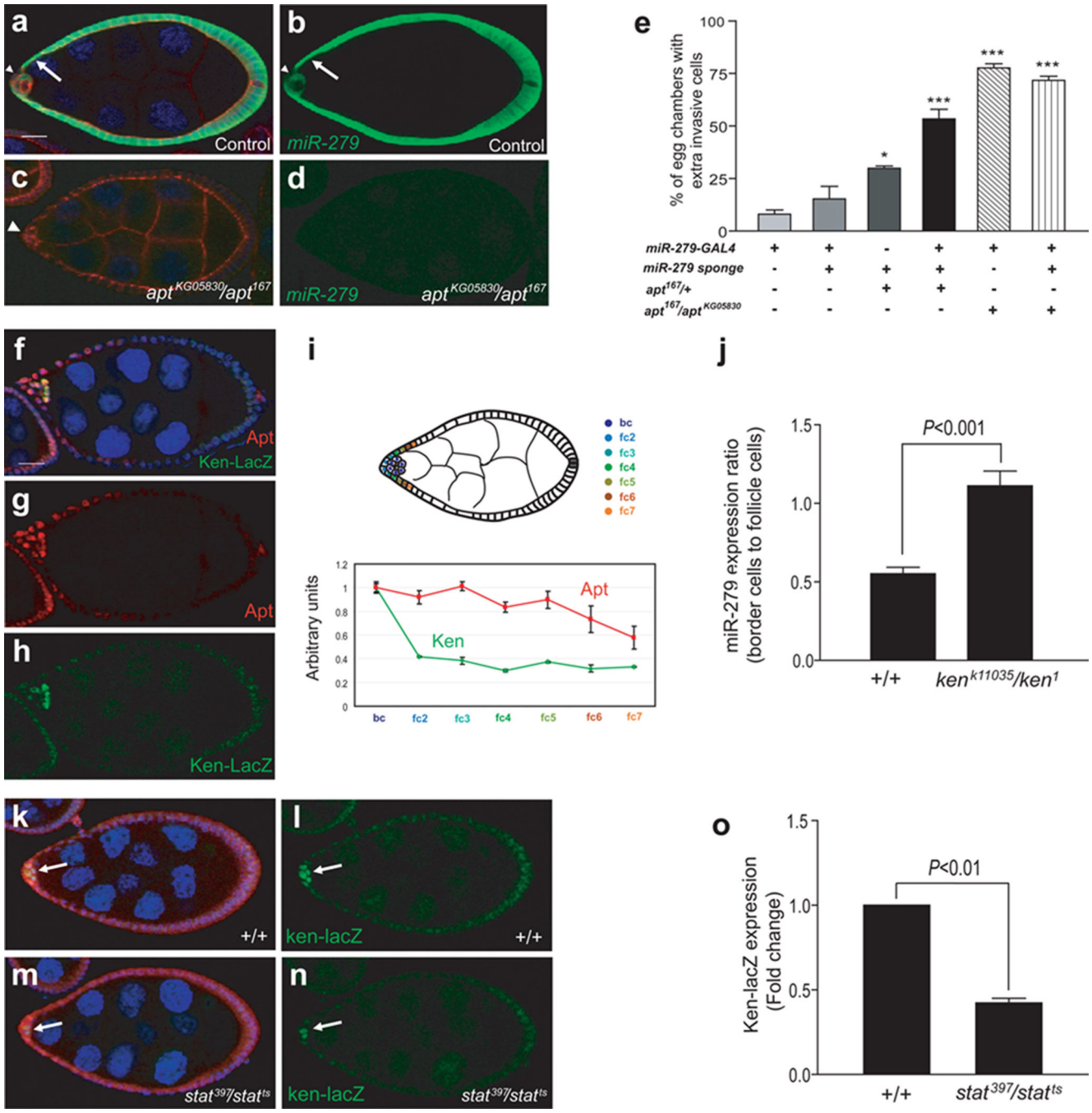

Figure 4. Two STAT targets, Apt and Ken, feed back via miR-279

(a–d) Confocal micrographs of stage 8 wild-type (a, b) or *apt* mutant background (*apt*^{KG05830}/*apt*^{167}) (c, d) egg chambers carrying a *miR-279* expression reporter (*miR-279-GAL4; UAS-GFP*). DAPI (blue) labels nuclei, and Armadillo (red) labels membranes enriched in adherens junction proteins. Arrowheads indicate the border cell cluster and arrows indicate non- migratory anterior follicle cells. Scale bars represent 20 μ. (e) Quantification of egg chambers of the indicated genetic backgrounds displaying extra invasive cells. Error bars represent SEMs. P values were calculated using ANOVA.

*P<0.05, ***P<0.001 (f–i) Expression patterns of Apt and Ken in early stage 9 egg chambers (f–h) Confocal micrographs of early stage 9 egg chambers carrying a *ken* reporter expressing beta-galactosidase under the control of the *ken* locus (*PZ ken*^{1}) (f, h, green) also stained for Apt (f, g, red). Scale bars represent 20 μ. (i) Relative levels of nuclear staining intensity of each STAT target relative to DAPI staining intensity plotted as a function of distance from the polar cells. The border cells develop immediately next to the polar cells. Fc2 indicates the cell next to the border cells, fc3 the next cell, as indicated in the drawing (n=4, mean±SEM). (j) The ratio of *miR-279* expression in border cells to that in follicle cells in control and *ken* mutant (*ken*^{k11035}/*ken*^{1}) egg chambers at stage 8. (k–n) Confocal micrographs of stage 8 egg chambers carrying a ken expression reporter (*Ken-lacZ*) (green) in a wild-type (k, l) or *stat* mutant (*stat*^{397}/*stat*^{ts}) (m, n). DAPI (blue) labels nuclei, and STAT staining is shown in red. Arrows indicate border cells. (o) *Ken-lacZ* expression in control versus *stat* mutant border cells at the non-permissive temperature. Error bars represent SEM. P value was calculated using a Student's t test.

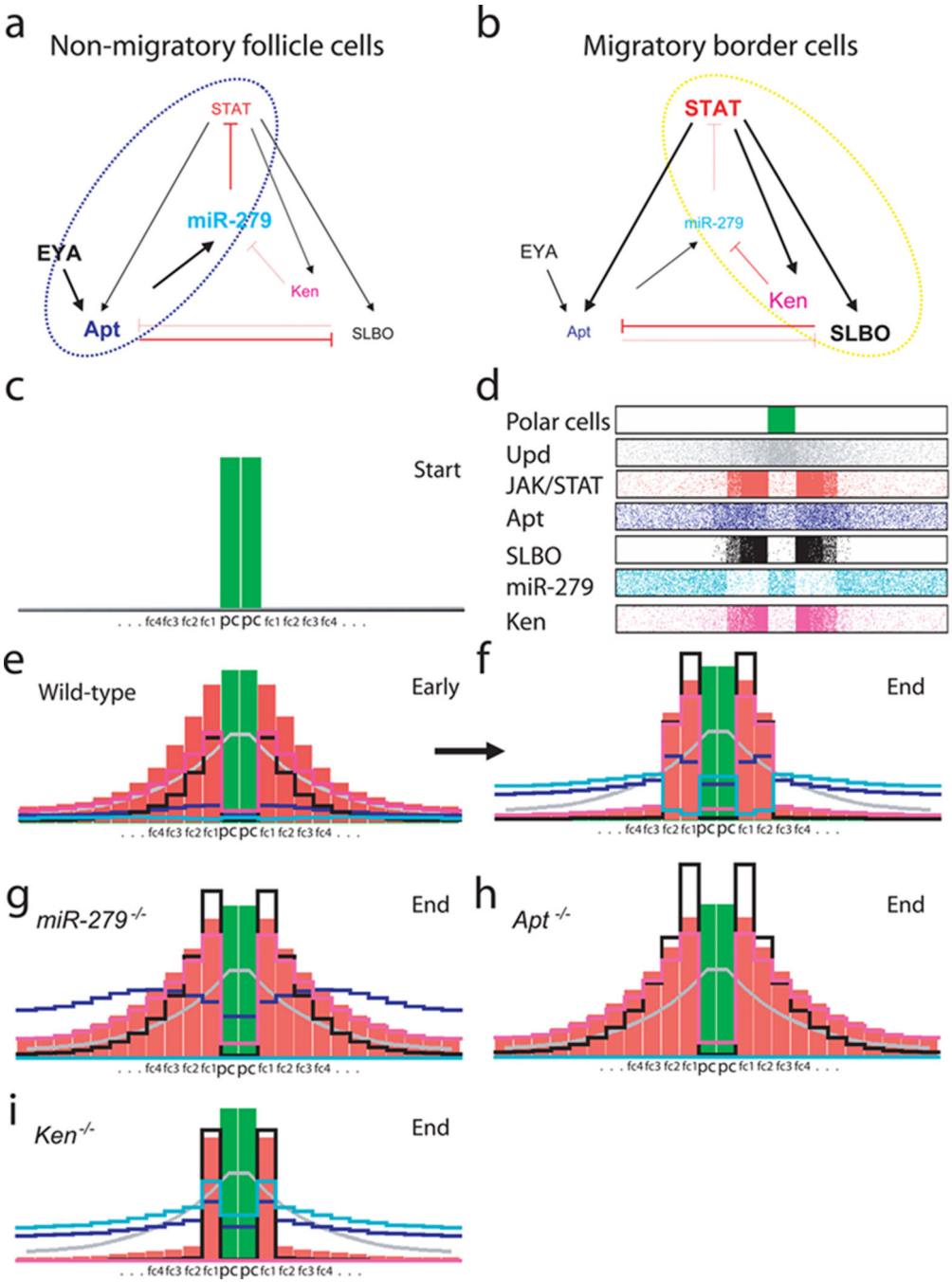

Figure 5. A model of the gene regulatory circuit required to specify non-migratory anterior follicle cell and migratory border cell fate

(a, b) Schematic model of the gene regulatory circuit including miR-279, STAT, Apt, Ken, and SLBO. (a)The blue circle highlights the negative feedback loop that represses STAT expression/activity in non-migratory follicle cells. (b) The yellow circle highlights the positive feedback loop amplifying STAT expression/activity in migratory border cells. Mutual repression of SLBO and Apt, and the effect of EYA on Apt are also indicated, as previously reported[4,21]. (c–i) Computer simulations based on the differential equations provided in the methods. (c) Initial condition: the polar cells (green) are specified. Fc1

indicates the follicle cell next to the polar cell (pc), fc2 the next cell, and so on. (d) Schematic representation of stable steady state protein distributions within the field of cells; pixel density corresponds to concentrations (for equations and parameters see methods and Supplementary information, Table1). (e–i) Representations of protein distributions in wild-type and indicated mutants. Height of the bars is proportional to protein concentration. (e) The distributions in wild-type at an early time point. (f) Wild-type distributions at a late time point, i.e. steady state. STAT, SLBO and Ken have all reached high levels near the polar cells and have decayed in the rest of the field. (g, h) This sharpening does not occur if either *miR-279* (g) or *apt* (h) is removed. (i) Loss of Ken does not prevent the threshold response.